

# Effects of correlated disorder on the magnetism of double exchange systems

G. Bouzerar<sup>1,2</sup> and O. Cépas<sup>3</sup>

1. Institut Néel, département MCBT, 25 avenue des Martyrs, C.N.R.S., B.P. 166 38042 Grenoble Cedex 09, France
2. Institut Laue Langevin, BP156, 38042 Grenoble Cedex, France.
3. Laboratoire de physique théorique de la matière condensée, C.N.R.S. UMR 7600, Université Pierre-et-Marie-Curie, Paris, France.

(Dated: May 10, 2018)

We study the effects of short-range correlated disorder arising from chemical dopants or local lattice distortions, on the ferromagnetism of 3d double exchange systems. For this, we integrate out the carriers and treat the resulting disordered spin Hamiltonian within local random phase approximation, whose reliability is shown by direct comparison with Monte Carlo simulations. We find large scale inhomogeneities in the charge, couplings and spin densities. Compared with the homogeneous case, we obtain larger Curie temperatures ( $T_C$ ) and very small spin stiffnesses ( $D$ ). As a result, large variations of  $\frac{D}{T_C}$  measured in manganites may be explained by correlated disorder. This work also provides a microscopic model for Griffiths phases in double exchange systems.

The interest for disordered magnetic systems such as thin magnetic films of transition metal alloys (Fe-Ni,Co-Ni,...), diluted magnetic semiconductors (Ga<sub>1-x</sub>Mn<sub>x</sub>As,Ge<sub>1-x</sub>Mn<sub>x</sub>...), d<sup>0</sup> materials (HfO<sub>2</sub>,CaO,...) or manganites (Re<sub>x</sub>A<sub>1-x</sub>MnO<sub>3</sub>, where Re is a rare-earth ion and A an alkaline ion) has considerably increased during this last decade. One of the reasons is the potential of some of the materials to be incorporated in technological devices. Some of them play a very special role: systems which contain large scale inhomogeneities. Inhomogeneities can appear during the growth of the sample by molecular beam epitaxy for example but can also result from the interplay between many degrees of freedom (charge, spin, orbital, phonons). This is for example the case in manganites. It is known that manganites are strongly inhomogeneous at the nanometer scale: (i) large-scale structures in the *charge* density were seen by electron diffraction of thin films [1], or tunneling spectroscopy [2]; (ii) evidence for inhomogeneous *spin* density was found in neutron diffuse scattering [3], or NMR [4]; (iii) localized spin waves also suggest the presence of confining potentials [5]. There are also clear evidences of inhomogeneous structures above  $T_C$ , which were interpreted [6, 7] as a Griffiths phase [8]. Their microscopic origin is one of the central issues of the physics of manganites; it includes phase separation frustrated by long-range Coulomb interaction [9], chemical disorder [10, 11], polarons [12, 13].

In this paper, we argue that the way the disorder is modelled is important to understand large-scale inhomogeneous structures in 3d and to explain the Griffiths phase [6]. For this we consider a model where the disorder is *correlated* at short distances. This model gives a possible explanation for the broad and multi-modal distribution of NMR lines [4], or the wide distribution of Curie temperatures  $T_C$  [14] and spin stiffnesses [15] measured in different materials for the same carrier density. The microscopic origin of the correlated disorder could be

chemical or polaronic. For instance, in Re<sub>1-x</sub>A<sub>x</sub>MnO<sub>3</sub> the dopant A<sup>2+</sup> which substitutes Re<sup>3+</sup> creates a strong Coulomb potential on its neighborhood and in particular on the eight nearest neighbor Mn sites surrounding it [16]. This is the model of “color-centers” initially discussed by de Gennes [10]. Alternatively, local Jahn-Teller distortions can also be seen as a source of correlated disorder through “cooperative phonons”, which can be mapped onto the same model.

The 3d correlated disordered double exchange Hamiltonian we consider reads,

$$H = \sum_{ij\sigma} (t_{ij} c_{i\sigma}^\dagger c_{j\sigma} + h.c.) - J_H \sum_i \vec{S}_i \cdot \vec{s}_i + \sum_i \epsilon_i n_i \quad (1)$$

where  $t_{ij} = -t$  for nearest neighbors only,  $\vec{S}_i$  is a classical spin localized at site  $i$  ( $|\vec{S}_i| = 1$ ) and  $\vec{s}_i = c_{i\alpha}^\dagger (\vec{\sigma})_{\alpha\beta} c_{i\beta}$ ,  $J_H$  is the Hund coupling which is set to be  $\infty$ . The on-site potentials  $\epsilon_i$  may correspond, in particular, to the chemical substitution of Re<sup>3+</sup> by A<sup>2+</sup> defined by  $\epsilon_i = \epsilon_D \sum_l x_l^i$ ; where the sum runs over the  $l$  nearest neighbour cations of the Mn site  $i$  ( $l = 1, \dots, 8$ ), and  $\epsilon_D$  is the strength of the disorder. We choose randomly  $x$  cationic sites for A for which  $x_l^i = 1$  (otherwise  $x_l^i = 0$ ). We emphasize that the disorder is correlated because one dopant affects simultaneously the 8 nearest neighbour Mn sites. With these definitions  $\epsilon_i$  takes the discrete values 0,  $\epsilon_D$ ,  $2\epsilon_D, \dots, 8\epsilon_D$ . From stoichiometry, we would expect the hole density,  $n_h$  to be equal to  $x$ , but in order to include the local Jahn-Teller distortion picture as well, we allow them to be different.

The approach we use to study this model is in two steps. First, for a given configuration of disorder we diagonalize (1) in the real space, assuming a fully polarized ground-state at zero temperature. This allows to define an effective Heisenberg Hamiltonian for the classical spins,  $H_{\text{eff}} = \sum_{\langle ij \rangle} J_{ij} \vec{S}_i \cdot \vec{S}_j$ , where the disordered couplings  $\{J_{ij}\}$  are explicitly calculated in the limit  $J_H \rightarrow \infty$ , using  $J_{ij} = t_{ij} \langle c_{i,\uparrow}^\dagger c_{j,\uparrow} \rangle / 2$  [17, 18]. In the

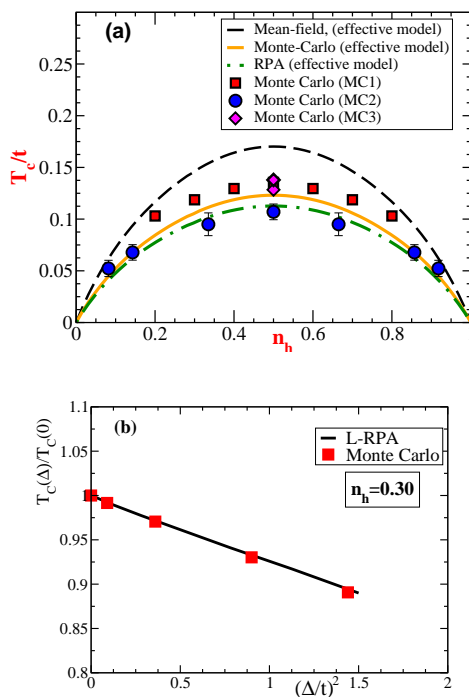


FIG. 1: (Color online) (a)  $T_C$  as a function of hole density (clean case). Lines are obtained with the effective Heisenberg Hamiltonian within Mean Field (dashed), RPA (dotted dashed) and Monte Carlo (continuous) treatments; and symbols from Monte Carlo simulations of the full double exchange model: MC1 [23], MC2 [20] and MC3 [22]. (b)  $T_C$  as a function of the on-site potential width  $\Delta$  for the Anderson disorder (*uncorrelated*): The continuous line is obtained with Local RPA and symbols are from Monte Carlo [23].

second step, we diagonalize this Hamiltonian using the self-consistent local random phase approximation (SC-LRPA)[19]. It consists of decoupling higher-order spin-spin Green's functions in the equation of motion. This introduces the local magnetizations  $\langle S_i^z \rangle$ , which are self-consistently determined by using sum rules. Spatial fluctuations due to disorder are thus treated exactly by solving the equations numerically in real space. This procedure was shown to be reliable to study dilute magnetic semiconductors where the couplings were calculated *ab initio* [19]. SC-LRPA provides an analytical expression for  $T_C$  and allows us to study much larger systems than those used in Monte Carlo.

In Fig. 1, we test this method by comparing  $T_C$  with that of Monte Carlo simulations for both the clean system ( $\epsilon_i = 0$ ) [20, 21, 22, 23] and the system with Anderson disorder [23, 24]. In the later case,  $\epsilon_i$  are *uncorrelated* variables uniformly distributed within  $[-\frac{\Delta}{2}, \frac{\Delta}{2}]$ . In Fig. 1a (clean case), the lines are obtained by studying  $H_{\text{eff}}$  within a simple mean-field theory,  $T_C^{MF} = 2J$  (dashed line), RPA,  $T_C^{RPA} = 1.32J$  [25] (dotted dashed line) and Monte Carlo,  $T_C^{MC} = 1.44J$  [26] (full line);

$J = \frac{-1}{2z} \frac{\langle K \rangle}{N}$  where the kinetic energy  $\langle K \rangle$  depends on  $n_h$ . For the clean system, we remind that  $T_C^{RPA} = 1.32J$  is obtained analytically using  $T_C^{RPA} = \frac{1}{3} (\sum_{\mathbf{q}} \frac{1}{E(\mathbf{q})})^{-1}$ , where  $E(\mathbf{q}) = zJ(1 - \gamma(\mathbf{q}))$  is the magnon dispersion,  $z$  the coordination number, and  $\gamma(\mathbf{q}) = \frac{1}{z} \sum_{\mathbf{r}_i} e^{i\mathbf{q} \cdot \mathbf{r}_i}$  [25]. This expression actually gives a very good approximation of  $T_C$ ; the error compared to Monte-Carlo is 8%. Now, the comparison with Monte-Carlo simulations of the full double exchange model (symbols) shows that the difference is within 10%, so that the two step approach is quantitatively reliable. Similarly, when Anderson disorder is added, we have found that SC-LRPA gives an excellent agreement with Monte Carlo data (Fig. 1b), stressing that not only the thermal fluctuations are well treated but also the spatial fluctuations due to disorder.

From now, we consider the model with *correlated* disorder, as discussed above. In Fig. 2a, 2b, 2c, we have plotted the magnetic couplings  $J_{ij}$  in a given layer for various hole densities ( $n_h = 0.1, 0.3$  and  $0.5$ , respectively). They are calculated for a fixed concentration of randomly distributed impurities (color centers),  $x = 0.3$ , and for a disorder strength,  $\epsilon_D = 0.15 W$  ( $W = 12 t$  is the bandwidth), that is chosen to be compatible with *ab initio* calculations [16]. At *low density* (Fig. 2a), the couplings are extremely inhomogeneous in space: we observe large clusters of strong couplings, embedded in regions of weak couplings. The distribution function of  $\{2J_{ij}\}$  (not shown) is peaked at  $\approx -0.003t$  but has a very long tail up to a cutoff at  $-0.3t$  (the average is  $\bar{J} = -0.02t$ ). The

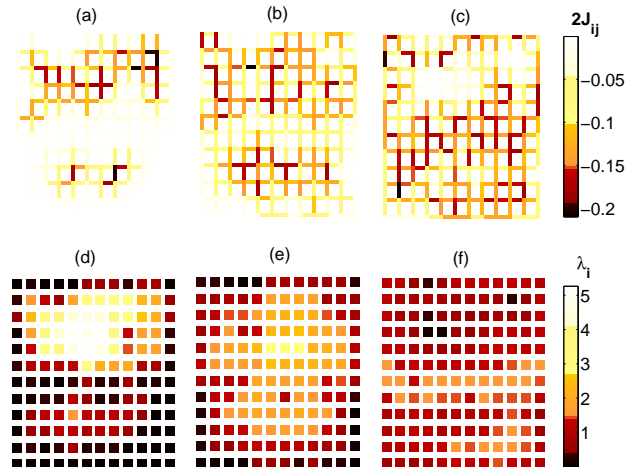


FIG. 2: (Color online.) Top row: real space picture of the magnetic couplings  $2J_{ij}$  of the effective model (*correlated disorder*), on one layer of the  $12^3$  cube. The dark (resp. white) regions correspond to large (resp. weak) couplings. Bottom row: real space distribution of  $\lambda_i = \lim_{T \rightarrow T_C} \frac{\langle S_i^z \rangle}{m}$  on the same layer. From left to right,  $n_h = 0.1$  (a),(d),  $0.3$  (b),(e) and  $0.5$  (c),(f). Parameters are  $x = 0.3$  and  $\epsilon_D = 0.15W$ .

regions of strong couplings correspond to hole rich regions with metallic properties embedded in a hole poor

matrix which is expected to be insulating, thus leading to phase separation. This tendency will be reinforced if antiferromagnetic superexchange couplings are taken into account, the hole poor regions will become antiferromagnetic or canted, as observed at very low dopings (droplets in a canted matrix) [3]. For Anderson disorder, we do not have well-defined nanoscale regions in 3d [24], unless cooperative phonons were included [27]. As the concentration of holes increases, the size of the regions of large couplings increases, and the system becomes less inhomogeneous. In this respect, close to half filling ( $n_h = 0.5$ ), the nature of the disorder becomes less important, as we shall see. The reason is that carriers with short Fermi wave length are less sensitive to the details of the disorder. Spatial inhomogeneities in the magnetization near  $T_C$  are directly seen in the distribution of  $\lambda_i = \lim_{T \rightarrow T_C} \frac{\langle S_i^z \rangle}{m}$ , where  $m$  is the averaged magnetization (Fig. 2). For a nearly homogeneous state,  $\lambda_i$  is close to 1, as seen in Fig. 2f. At low densities, we see a very inhomogeneous texture of  $\lambda_i$  (Fig. 2d), with local droplets with  $\lambda_i$  as high as  $\approx 4-5$ , surrounded by a region with very small local magnetizations. In this case, the distribution of the magnetizations is multi-modal. In between (Fig. 2b), the droplet increases in size and  $\lambda_i \approx 2$  is reduced with respect to Fig. 2a, the distribution has only one broad peak. These results resemble NMR results where multimodal distributions occur at low dopings and get broader for higher doping [4].

In Fig. 3, we give  $T_C$  averaged over at least 100 disorder configurations (symbols). To see clearly the role of the inhomogeneities, we have also indicated what  $T_C$  would be if we replace all couplings by their average, defined by  $\bar{J} = \frac{1}{zN} \sum_{ij} J_{ij} = \langle J_{ij} \rangle_{dis}$  (lines). The results are almost identical for  $n_h$  close to 0.5 but strongly differ otherwise. Similarly we have found (not shown) that for Anderson disorder,  $T_C$  is also extremely close to that of the homogeneous system calculated with  $\bar{J}$ . However, at lower hole densities where the couplings are strongly inhomogeneous (Fig. 2a), we observe that  $T_C$  is larger than that of the homogeneous sample. This happens because of the competition between large (percolating) clusters with couplings much stronger than  $\bar{J}$  that tend to increase  $T_C$  and thermal fluctuations that reduce it. In particular, at  $n_h = 0.1$ ,  $T_C$  happens to be close to the mean-field result  $T_C^{MF} = 2\bar{J}$  (dashed line), as the result of this competition. It is interesting to remark that this picture is different from the pure percolation picture where thermal fluctuations in the clusters wins and reduce  $T_C$ ; the difference is that the distribution is much more inhomogeneous here. We note that our  $T_C$  are much smaller than that obtained in ref. [28], where the same model was studied. The reason is that here both spatial and thermal fluctuations are treated beyond mean-field virtual crystal approximation.

We now argue that this model gives grounds for a Griffiths phase [6, 8] above  $T_C$ . As discussed in ref. [7],

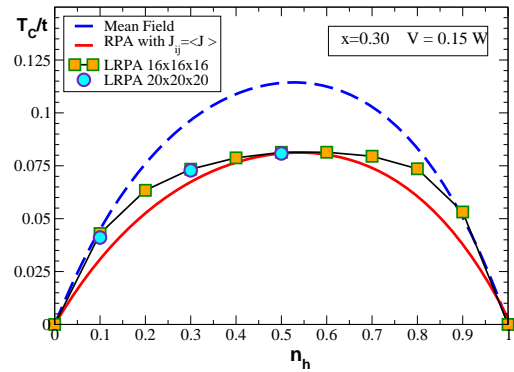


FIG. 3: (Color online.)  $T_C$  (symbols) as a function of hole density for the model with correlated disorder calculated by SC-LRPA (averaged over 100 configurations of disorder). Also given are the mean-field (dashed line), RPA with all couplings identical  $J_{ij} = \bar{J}$  (continuous line). Parameters are  $x = 0.3$  and  $\epsilon_D = 0.15W$ . Calculations are done for sizes  $16^3$  and  $20^3$ .

correlations in the disorder should enhance the Griffiths phenomenon. Indeed, it is more likely to find large clusters with higher local “Curie” temperatures, as seen in Fig. 2a. We calculate this temperature  $T_G$  from the lowest eigenvalue  $\epsilon$  of  $J_{ij}$ , using  $T_G = \frac{1}{3}S(S+1)|\epsilon|$  [8]. Since this is a mean field estimation,  $T_G$  has to be compared to  $T_C^{MF}$ . For  $n_h = 0.1$ , we find a large  $T_G = 0.11t \approx 2.5T_C^{MF}$ . On the other hand, for  $n_h \sim 0.5$ , the couplings are much more homogeneous, and we have found a much smaller region for the Griffiths phase with  $T_G = 0.13t \approx T_C^{MF}$ . This is interesting because it shows that  $T_G$  is weakly sensitive to  $n_h$ . Experimentally this phase seems to occur only in the structurally distorted phase at low dopings [7], which suggests that the origin of correlated disorder is the local Jahn-Teller distortions, a case that is also covered by the present model. In fact it is not clear from our study that we can exclude the chemical origin of the correlated disorder because the Griffiths phase shrinks as we increase the carrier density. A better treatment of thermal fluctuations could possibly lead to the complete disappearance of the Griffiths phase for larger dopings.

We now discuss the effect of the inhomogeneities on the long wave length spin excitations at zero temperature. Even in the presence of disorder, these excitations are well defined and characterized by a spin stiffness  $D$  [18, 29], that is calculated following [29]. Experiments on various manganites show that the dimensionless ratio  $D/a^2 T_C$  ( $a$  is the lattice constant, taken to be 1 in the following) strongly varies with doping and takes values as small as 0.05 and up to 0.5 [15]. This is in contrast with the *clean* double exchange model, where  $D/T_C$  is a constant equal to 0.755 (RPA for the s.c. lattice [25]), independent of the hole density. We argue that the measured small values could be explained with the model of

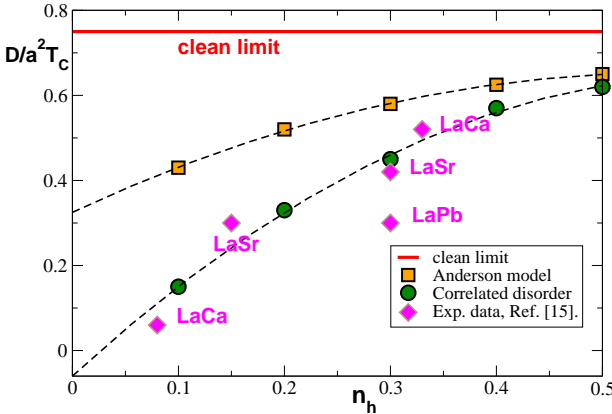


FIG. 4: (Color online.) Dimensionless ratio  $D/a^2 T_C$  of the spin stiffness to the Curie temperature as a function of the hole density  $n_h$ , for the correlated and Anderson forms of disorder. The width of the distribution of potentials was chosen to be the same in both cases:  $\epsilon_D = 0.15W$  ( $x = 0.3$ ) and  $\Delta = 0.80W$ . Experimental results [15] are divided by the lattice constant of  $\text{LaMnO}_3$  squared ( $a = 3.9\text{\AA}$ ).

correlated disorder, but would require unrealistic large strength of the disorder in the uncorrelated case. Fig. 4 gives this ratio, calculated for both models of disorder. Note that to allow for a direct comparison, the width of the distributions of  $\epsilon_i$  is chosen to be the same. Close to  $n_h = 0.5$ ,  $D/T_C$  does not really depend on the model, reflecting the absence of the large scale inhomogeneities we discussed above. When  $n_h$  decreases, however, the spin stiffness is dominated by large regions of weak couplings (Fig. 2a): at  $n_h = 0.10$ ,  $D/T_C$  is 3 times smaller than that obtained with Anderson disorder. In order to get such small values in the Anderson disordered case, one would need a value of  $\Delta$  much larger than the bandwidth, which would be difficult to reconcile with *ab initio* estimations [16], on one hand, and would tend to localize all carriers [24] on the other hand. In Fig. 4 we have also compared our calculations directly with available experimental values [15]. First we note that the overall quantitative agreement does not mean that  $\epsilon_D$  is quantitatively determined for manganites because other interactions have been neglected here (there is anyway a distribution of ratios for a same doping, see LaSr and LaPb in Fig. 4, for instance which could be explained by different  $\epsilon_D$ ). Nevertheless, it is interesting to see that the trend as function of the hole density is already well captured by taking disorder into account, and that a relatively small amount of *correlated* disorder leads to very small values of  $D/T_C$ , contrary to what would be needed in the Anderson case.

To conclude, we have found that short-range correlated disorder creates large scale spin and charge textures, particularly inhomogeneous at low dopings. Our study suggests that describing the disorder in a more realistic manner may be a key point to understand experiments, as the

occurrence of a Griffiths phase observed for low dopings. In addition, we have found that correlations in the disorder tend to increase  $T_C$  because of the presence of large clusters of strong couplings, and decrease the spin stiffness  $D$ . This results in very small ratios  $D/T_C$ , consistent with what has been measured in manganites but hardly compatible with Anderson disorder. The dimensionless ratio  $D/T_C$  appears as a good measure of the inhomogeneous character of the magnetic state, a conclusion that may apply beyond manganese oxides.

We thank M. Clusel, M. Hennion, P. Majumdar, Y. Motome, F. Moussa and S. Petit for stimulating discussions. O. C. thanks the ILL for hospitality.

---

- [1] M. Uehara, S. Mori, C.H. Chen and S.W. Cheong, *Nature* **399**, 560 (1999).
- [2] M. Fäth, S. Freisem, A. A. Menovsky, Y. Tomioka, J. Aarts and J. A. Mydosh, *Science* **285**, 1540 (1999).
- [3] M. Hennion, F. Moussa, G. Biotteau, J. Rodríguez-Carvajal, L. Pinsard, and A. Revcolevschi, *Phys. Rev. Lett.* **81**, 1957 (1998).
- [4] G. Allodi, R. De Renzi, and G. Guidi, *Phys. Rev. B* **57**, 1024 (1998); G. Papavassiliou, M. Pissas, G. Diamantopoulos, M. Belesi, M. Fardis, D. Stamopoulos, A. G. Kontos, M. Hennion, J. Dolinsek, J.-Ph. Ansermet and C. Dimitropoulos, *Phys. Rev. Lett.* **96**, 097201 (2006).
- [5] M. Hennion, F. Moussa, P. Lehuelleur, F. Wang, A. Ivanov, Y. M. Mukovskii and D. Shulyatev, *Phys. Rev. Lett.* **94**, 057006 (2005).
- [6] M. B. Salamon, P. Lin, and S. H. Chun, *Phys. Rev. Lett.* **88**, 197203 (2002); P. Y. Chan, N. Goldenfeld, and M. Salamon, *Phys. Rev. Lett.* **97**, 137201 (2006).
- [7] J. Deisenhofer, D. Braak, H.-A. Krug von Nidda, J. Hemberger, R. M. Eremina, V. A. Ivashin, A. M. Balbashov, G. Jug, A. Loidl, T. Kimura and Y. Tokura, *Phys. Rev. Lett.* **95**, 257202 (2005).
- [8] A. J. Bray, *Phys. Rev. Lett.* **59**, 586 (1987).
- [9] A. Moreo, S. Yunoki, E. Dagotto, *Science* **283**, 2034 (1999); E. Dagotto, *Nanoscale phase separation and colossal magnetoresistance* (Springer, Berlin 2002).
- [10] P.-G. de Gennes, *Phys. Rev.* **118**, 140 (1960).
- [11] E. L. Nagaev, *Phys. Rep.* **346**, 387 (2001).
- [12] T. V. Ramakrishnan, H. R. Krishnamurthy, S. R. Hassan, and G. Venkateswara Pai, *Phys. Rev. Lett.* **92** 157203 (2004).
- [13] V. B. Shenoy, T. Gupta, H. R. Krishnamurthy and T. V. Ramakrishnan, *Phys. Rev. Lett.*, **98**, 097201 (2007).
- [14] H. Y. Hwang, S-W. Cheong, P. G. Radaelli, M. Marezio and B. Batlogg, *Phys. Rev. Lett.* **75**, 914 (1995).
- [15] J. A. Fernandez-Baca, P. Dai, H. Y. Hwang, C. Kloc, and S-W. Cheong, *Phys. Rev. Lett.* **80**, 4012 (1998), and references therein; see also T. Chatterji, L. P. Regnault, P. Thalmeier, R. van de Kamp, W. Schmidt, A. Hiess, P. Vorderwisch, R. Suryanarayanan, G. Dhalenne and A. Revcolevschi, *J. Alloys Compd.* **326**, 15 (2001).
- [16] W. E. Pickett and D. Singh, *Phys. Rev. B* **55**, R8642 (1997).
- [17] K. Kubo and N. Ohata, *J. Phys. Soc. Jpn.* **33** 21(1972).
- [18] Y. Motome and N. Furukawa, *Phys. Rev. B* **71**, 014446

(2005).

[19] G. Bouzerar, T. Ziman, and J. Kudrnovsky, *Europhys. Lett.* **69**, 812 (2005).

[20] S. Yunoki, J. Hu, A. L. Malvezzi, A. Moreo, N. Furukawa and E. Dagotto, *Phys. Rev. Lett.* **80**, 845 (1998).

[21] M. J. Calderon and L. Brey, *Phys Rev B* **58**, 3286 (1998).

[22] J. L. Alonso, L. A. Fernández, F. Guinea, V. Laliena, and V. Martín-Mayor, *Nucl. Phys. B* **596**, 587 (2001).

[23] Y. Motome and N. Furukawa, *Phys. Rev. B* **68**, 144432 (2003).

[24] S. Kumar and P. Majumdar, *Phys. Rev. Lett.* **91**, 246602 (2003).

[25] H. B. Callen, *Phys Rev* **130**, 890 (1963).

[26] K. Chen, A. M. Ferrenberg, and D. P. Landau, *Phys. Rev. B* **48**, 3249 (1993).

[27] S. Kumar, A. P. Kampf, and P. Majumdar, *Phys. Rev. Lett.* **97**, 176403 (2006).

[28] J. Salafranca and L. Brey, *Phys. Rev. B* **73**, 214404 (2006).

[29] G. Bouzerar, *cond-mat/0610465* (unpublished).